Indole-3-propionic acid alleviates intestinal epithelial cell injury via regulation of the TLR4/NF-κB pathway to improve intestinal barrier function

YING CHEN[1,2*], YU LI[2*], XIAOJUAN LI[2], QINGQING FANG[2], FENG LI[2,3], SHIYAO CHEN[2,3] and WEICHANG CHEN[1]

[1]Department of Gastroenterology, The First Affiliated Hospital of Soochow University, Suzhou, Jiangsu 215000, P.R. China; [2]Department of Gastroenterology and Hepatology, Minhang Hospital, Fudan University, Shanghai 201100, P.R. China; [3]Department of Gastroenterology and Hepatology, Zhongshan Hospital, Fudan University, Shanghai 200032, P.R. China

Received March 29, 2024; Accepted July 12, 2024

DOI: 10.3892/mmr.2024.13313

Abstract. Indole-3-propionic acid (IPA), a product of *Clostridium sporogenes* metabolism, has been shown to improve intestinal barrier function. In the present study, *in vitro* experiments using NCM460 human colonic epithelial cells were performed to investigate how IPA alleviates lipopolysaccharide (LPS)-induced intestinal epithelial cell injury, with the aim of improving intestinal barrier function. In addition, the underlying mechanism was explored. NCM460 cell viability and apoptosis were measured using the Cell Counting Kit-8 assay and flow cytometry, respectively. The integrity of the intestinal epithelial barrier was evaluated by measuring transepithelial electrical resistance (TEER). The underlying molecular mechanism was explored using western blotting, immunofluorescence staining, a dual luciferase reporter gene assay and quantitative PCR. The results showed that 10 μg/ml LPS induced the most prominent decrease in cell viability after 24 h of treatment. By contrast, IPA effectively inhibited LPS-induced apoptosis in the intestinal epithelial cells. Additionally, >0.5 mM IPA improved intestinal barrier function by increasing TEER and upregulating the expression of tight junction proteins (zonula occludens-1, claudin-1 and occludin). Furthermore, IPA inhibited the release of pro-inflammatory cytokines (IL-1β, IL-6 and TNF-α) in a dose-dependent manner and this was achieved via regulation of the Toll-like receptor 4 (TLR4)/myeloid differentiation factor 88/NF-κB and TLR4/TRIF/NF-κB pathways. In conclusion, IPA may alleviate LPS-induced inflammatory injury in human colonic epithelial cells. Taken together, these results suggest that IPA may be a potential therapeutic approach for the management of diseases characterized by LPS-induced intestinal epithelial cell injury and intestinal barrier dysfunction.

Correspondence to: Professor Weichang Chen, Department of Gastroenterology, The First Affiliated Hospital of Soochow University, 899 Pinghai Road, Suzhou, Jiangsu 215000, P.R. China
E-mail: weichangchen@126.com

Professor Shiyao Chen, Department of Gastroenterology and Hepatology, Minhang Hospital, Fudan University, 170 Xinsong Road, Shanghai 201100, P.R. China
E-mail: syaochen@fudan.edu.cn

*Contributed equally

Abbreviations: IPA, indole-3-propionic acid; TEER, transepithelial electrical resistance; TJ, tight junction; LPS, lipopolysaccharide; TLR4, Toll-like receptor 4; MyD88, myeloid differentiation factor 88

Key words: IPA, pro-inflammatory cytokine, intestinal epithelial barrier, LPS, TJ proteins

Introduction

The intestinal microenvironment is a highly complex and dynamic system, wherein the maintenance of the intestinal barrier serves a pivotal role in preserving the structural integrity of the intestines (1). Consisting of the mucous layer, intercellular tight junction (TJ) proteins and epithelial cells, the intestinal epithelial barrier acts as a robust defense mechanism, protecting against tissue damage and the onset of various diseases, such as inflammatory bowel disease and colitis (2). Perturbations in the microbial ecosystem of the intestines frequently increase intestinal permeability and induce intestinal epithelial dysfunction (3). Lipopolysaccharide (LPS), a constituent of the outer membrane of gram-negative bacteria, has been shown to exacerbate inflammatory responses by increasing the production of nitric oxide and pro-inflammatory cytokines in intestinal epithelial cells, specifically in NCM460 cells (4). Notably, higher levels of LPS are implicated in TJ disruption, compromised barrier integrity and perturbed epithelial cell turnover (5,6). Therefore, there is a crucial need to explore targeted therapeutic strategies for LPS-induced intestinal epithelial dysfunction.

A previous study indicated that indole possesses anti-inflammatory properties, and positively affects gastrointestinal tract and liver homeostasis (7). Of the intestinal microorganisms, *Clostridium sporogenes* is responsible for the

production of indole-3-propionic acid (IPA) (8,9). IPA has been shown to serve as a biomarker of disease remission for active colitis, since a gradual restoration of serum IPA level has been detected during the recovery phase (10). Notably, IPA serves a crucial role in strengthening mucus and mechanical barriers by promoting TJ expression, thereby enhancing barrier function (11,12). While the role of IPA in preserving the intestinal barrier has been established, a comprehensive understanding of its mechanisms of action on intestinal epithelial cells is still lacking.

Toll-like receptor 4 (TLR4) dependent on myeloid differentiation factor 88 (MyD88) and the downstream NF-κB signaling pathway is essential for the induction of inflammation (13). YIt has been observed that gut microbial diversity affects the TLR4/NF-κB signaling pathway during an inflammatory response. LPS rapidly increases cytokine levels, impairing intestinal integrity in intestinal epithelial cells (14). Furthermore, activation of TLR4 by LPS initiates signaling via either MyD88 or TRIF, resulting in the translocation of nuclear transcription factors NF-κB, AP-1 and IRF3 (15). Nuclear stimulation by LPS activates the MyD88-dependent and downstream NF-κB signaling pathway, compromising intestinal barrier function (16). Previous studies have suggested that IPA exhibits beneficial effects in regulating immune responses within the intestines via activation of the aryl hydrocarbon receptor and the pregnane X receptor ligands (17,18). Furthermore, IPA effectively has been shown to protect against LPS-induced C2C12 cell inflammation (19). However, the precise mechanisms underlying the protective effects of IPA on LPS-induced epithelial intestinal cell injury are currently unclear.

The effects of IPA on intestinal barrier function have been reported in few studies, most of which used the Caco-2 cell line (11,20), whereas the effects on the NCM460 cell line have rarely been reported. Furthermore, the NCM460 cell line has been used in cutting-edge research, such as that associated with infectious diseases, cell signaling and cytokine production (4,21). Therefore, in the present study, the human NCM460 colonic epithelial cell line was used to explore the mechanisms by which IPA may protect against LPS-induced intestinal epithelial cell injury using three concentrations of IPA. The findings of the present study highlight novel avenues for the potential therapeutic role of IPA in intestinal inflammatory diseases characterized by LPS-induced intestinal epithelial cell injury.

Materials and methods

Reagents. IPA (>98%) was purchased from Shanghai Aladdin Biochemical Technology Co., Ltd. LPS was purchased from MilliporeSigma. Fetal bovine serum (FBS; cat. no. 16000-044) was purchased from Gibco (Thermo Fisher Scientific, Inc.) and DMEM (cat. no. BL304A) was purchased from Biosharp Life Sciences. The penicillin-streptomycin solution (100X; cat. no. P1400-100) and trypsin-EDTA (0.25%; cat. no. T1300-100) were obtained from Beijing Solarbio Science & Technology Co., Ltd. The Cell Counting Kit-8 (CCK-8) assay was purchased from Beyotime Institute of Biotechnology. Nuclease-Free Water (cat. no. 10601ES76), Diethylpyrocarbonate (DEPC; cat. no. 10602ES25), Hifair®II 1st Strand cDNA Synthesis Kit (cat. no. 11119ES60) and Hieff® quantitative (q)PCR SYBR Green MasterMix (cat. no. 11203ES03) were purchased from Shanghai Yeasen Biotechnology Co., Ltd. The BCA Protein Quantification Kit (cat. no. 23223) was purchased from Thermo Fisher Scientific, Inc. Alexa Fluor 488-labeled goat anti-rabbit IgG (H+L) (cat. no. A0423) and Annexin V-FITC Apoptosis Detection Kit (cat. no. C1062) were obtained from Beyotime Institute of Biotechnology The Dual-Luciferase Reporter Gene Assay Kit (cat. no. E1910) was purchased from Promega Corporation.

Cell culture. The NCM460 human colonic epithelial cell line was purchased from Shanghai Jinyuan Biotechnology Co., Ltd. The cells were cultured in DMEM supplemented with 10% FBS and 1% penicillin-streptomycin solution in an incubator at 37˚C supplied with 5% CO_2. NCM460 cells were treated with various concentrations of LPS with or without IPA for 3 or 24 h at 37˚C. The cells were grouped as follows: Untreated cells served as a control; LPS 10 μg/ml; LPS 10 μg/ml + IPA 0.05 mM; LPS 10 μg/ml + IPA 0.5 mM; and LPS 10 μg/ml + IPA 5 mM.

Measurement of cell viability. Cell viability was measured using the CCK-8 assay according to the manufacturer's protocol. Briefly, $5x10^3$ cells/well were plated in 96-well plates and treated with 0, 0.5, 1, 5 or 10 μg/ml LPS for 3 or 24 h at 37˚C. The concentration of LPS that best attenuated cell viability was used as the inducing concentration for the follow-up experiments. Subsequently, NCM460 cells were co-treated with LPS and 0.05, 0.5 or 5 mM IPA for 72 h at 37˚C. For the CCK-8 assay, 10 μl CCK-8 reagent was added to each well and incubated for 1 h at 37˚C. A microplate reader (cat. no. 9602G; Perlong Medical Equipment Co., Ltd.) was then used to measure the absorbance at a wavelength of 450 nm. Each experiment was repeated five times and the cell survival rate was calculated using the following formula: Cell viability (%)=(mean absorbance of test wells-mean absorbance of blank wells)/(mean absorbance of control wells-mean absorbance of blank wells) x100.

Detection of apoptosis. Apoptosis was detected using the Annexin V-FITC Apoptosis Detection Kit according to the manufacturer's protocol. Adherent cells seeded in a 6-well plate at a density of $5x10^5$/well were washed once with PBS and then digested using trypsin containing EDTA. After centrifugation at 1,000 x g for 5 min at 37˚C, the cells were collected and incubated with Annexin V-FITC (5 μl) for 15 min, followed by staining with propidium iodide (PI, 5 μl) staining solution for 5 min at 4˚C in the dark. A sample without Annexin V-FITC and PI staining was used as a negative control. Subsequently, cell apoptosis was detected using a flow cytometer (CytoFLEX; Beckman Coulter, Inc.) and data were analyzed using FlowJo software version 10.6.2 (Tree Star, Inc.) to determine the percentage of apoptotic cells, with Annexin V-FITC fluorescing green and PI fluorescing red. The total apoptotic rate was calculated as the sum of early apoptosis and late apoptosis. Each experiment was repeated three times and the mean apoptotic rate was calculated.

Assessment of barrier integrity. The Millicell®-ERS Voltohmmeter (MilliporeSigma) was used to assess barrier

integrity via measuring transmembrane electrical resistance (TEER). NCM460 cells were seeded in the upper chambers of a 24-well Transwell plate (diameter, 6.5 mm; pore size, 8.0 μm; cat. no. 3422; Costar; Corning Inc.) at a density of $2x10^5$ cells/cm^2, and were cultured in a 5% CO_2 incubator at 37˚C. The medium (DMEM; cat. no. SH30243.01; Hyclone; Cytiva) added in the lower chambers was changed every 3 days until the cells grew in a monolayer on the upper side of the polyester membrane, after which, the transmembrane resistance was measured. The resistance per unit area (TEER) was calculated using the following formula: TEER (resistance per unit area, $\Omega \cdot cm^2$)=($R_{experiment}$-R_{blank}) (resistance measurement, Ω) x effective membrane area (cm^2). The effective area of the Millicell membrane used was 0.6 cm^2. $R_{experiment}$ was the resistance of the membrane with a cell layer in each experimental group while R_{blank} was the resistance of the membrane without a cell layer. The TEER value was measured three consecutive times and the mean TEER value in each group was calculated.

Immunofluorescence staining. NCM460 cells were cultured and treated with the control medium, or medium containing 10 μg/ml LPS alone or alongside various concentrations of IPA (0.05, 0.5 or 5 mM). Cells were seeded onto 24-well round glass coverslips (14 mm; cat. no. WHB-24-CS; Beijing Solarbio Science & Technology Co., Ltd.) at a density of $3x10^4$ cells/well were washed with 0.02 M PBS to remove the media, fixed with 4% formaldehyde for 30 min and permeabilized with 0.5% Triton X-100 for 10 min at 37˚C. Slides were then blocked with 1% bovine serum albumin (cat. no. A8010; Beijing Solarbio Science & Technology Co., Ltd.) for 1 h at 37˚C and washed three times using 0.02 M PBS. Subsequently, the cells were incubated with the recombinant anti-ZO1 TJ protein antibody (rabbit monoclonal; 1:100; cat. no. ab221547; Abcam) overnight at 4˚C, followed by incubation with the fluorescent-tagged secondary antibody (1:200; cat. no. A0423; Beyotime Institute of Biotechnology). After washing with PBS, an anti-quenching solution containing DAPI (1:500 dilution) was used to seal the slides. Finally, images of three random fields of view were captured using a fluorescence microscope (magnification, x200). Semi-quantitative assessment of fluorescence intensity was performed using ImageJ software version 1.53a (National Institutes of Health). Mean fluorescence intensity was calculated using the following formula: Mean fluorescence intensity (AU)=Integrated density/area.

Reverse transcription (RT)-qPCR. Total RNA was extracted from cells using TRleasy™ Total RNA Extraction Reagent (cat. no. 10606ES60; Shanghai Yeasen Biotechnology Co., Ltd.), and was then isolated using chloroform, precipitated with isopropanol, washed with 75% ethanol and dissolved in DEPC water. The RNA was reverse transcribed into cDNA using Hifair® II 1st Strand cDNA Synthesis Kit (cat. no. 11119ES60; Shanghai Yeasen Biotechnology Co., Ltd.) according to the manufacturer's instructions. qPCR was performed using Hieff® qPCR SYBR Green Master Mix (cat. no. 11203ES03; Shanghai Yeasen Biotechnology Co., Ltd.) on a fluorescence qPCR instrument (cat. no. CG-05; Hangzhou Lattice Scientific Instrument Co., Ltd.). The qPCR conditions were set as follows: Pre-denaturation at 95˚C for 5 min, followed by 40 cycles of denaturation at 95˚C for 10 sec, annealing at 55-60˚C for 20 sec and extension at 72˚C for 20 sec. Fluorescence was detected and melting curve analysis was performed at the end of each PCR cycle to assess amplification specificity. The relative expression levels of the target genes were calculated using the $2^{-\Delta\Delta Cq}$ method (22), and β-actin was used as an internal reference. The mRNA expression levels of IL-1β, IL-6, TNF-α, TLR4, MyD88, TRIF and p65-NF-κB were detected in triplicate, and the sequences of the primers used are listed in Table SI.

Enzyme-linked immunosorbent assay (ELISA). The concentrations of proinflammatory cytokines IL-1β, IL-6 and TNF-α were quantified using ELISA kits (cat. nos. SDH0014-48T, SDH0021-48T, SDH0001-48T; Shanghai Siding Biotechnology Co., Ltd.) according to the manufacturer's instructions. The OD was detected using a microplate reader (Tecan Infinite F50; Tecan Group, Ltd.) at 450 nm. Concentrations were calculated by standard curve plotting.

Dual-luciferase reporter gene assay. Dual-luciferase reporter gene detection was performed using the Dual-Luciferase Reporter Gene Detection Kit (cat. no. E1910; Promega Corporation) according to the manufacturer's protocol. Cells in the logarithmic growth phase were digested with trypsin, and $5x10^5$ cells/well were plated in a 6-well plate and cultured for 24 h. The GV238 (pGL3 basic) vector plasmid and p65-NF-κB gene sequence were digested with *Kpn*I/*Xho*I restriction enzymes (Shanghai GeneChem Co., Ltd.). The p65-NF-κB gene promotor was obtained from the cDNA library of Shanghai GeneChem Co., Ltd. The primer sequences used to amplify the sequence were as follows: Forward, 5'-TTTCTCTATCGATAGGTACCGGGAATT TCCGGGGACTTTC-3' and reverse, 5'-CTTAGATCGCAG ATCTCGAGCTGGAAGTCGAGCTTCCATTATATAC-3'. Subsequently, the p65-NF-κB gene promotor was cloned into the GV238 vector to construct an overexpression vector, which was then transfected into NCM460 cells. NCM460 cells transfected with 1.5 μg luciferase-p65-NF-κB reporter plasmid and 1.5 μg *Renilla* control plasmid (cat. no. E1910; Promega Corporation). The transfection solutions were prepared according to the instructions of the transfection reagent Lipofectamine® 3000 (cat. no. L3000001; Invitrogen; Thermo Fisher Scientific, Inc.). After 48 h of transfection, the cells were washed once with PBS and cultured in 500 μl passive lysis buffer for 15 min. Subsequently, cells were treated with 10 μg/ml LPS alone, or alongside various concentrations of IPA (0.05, 0.5 or 5 mM) for 72 h at 37˚C. Afterwards the cells were collected and transferred to a 96-well microplate, and 100 μl luciferase assay reagent II and 20 μl passive lysis buffer were then added to detect firefly luciferase activity. The luciferase activity was detected by adding 100 μl Stop&Glo reagent and the ratio of the luciferase activity to *Renilla* luciferase activity was calculated.

Western blotting. Total proteins were extracted from cells lysed using RIPA lysis buffer (cat. no. P0038; Beyotime Institute of Biotechnology) and the supernatant was centrifuged at 16,000 x g for 15 min at 4˚C. Protein concentrations were measured using the BCA Protein Quantification Kit according to the manufacturer's instructions. Subsequently, ~20 μg total

protein was separated by SDS-PAGE on 10% gels and transferred to PVDF membranes at 25 V for 30 min. The membranes were then blocked with 5% non-fat milk solution at 4˚C overnight and incubated with the following antibodies at 4˚C overnight: β-actin (1:5,000; cat. no. 81115-1-R; Proteintech Group, Inc.), zonula occludens (ZO)-1 (1:1,000; cat. no. ab276131; Abcam), occludin (1:1,000; cat. no. ab216327; Abcam), Claudin-1 (1:2,000; cat. no. ab211737; Abcam) p65-NF-κB (1:1,000; cat. no. ab32536; Abcam) and phosphorylated-p65-NF-κB (1:1,000; cat. no. ab76302; Abcam). After washing, the membranes were incubated with HRP-labeled secondary antibodies (1:10,000; cat. no. ZB-2301; OriGene Technologies, Inc.) for 1 h at 37˚C. The membranes were washed three times in Tris-buffered saline-0.1% Tween 20 (5 min/wash) between each incubation step. For visualization, ECL solution (cat. no. WBKLS0100; MilliporeSigma) was prepared according to the manufacturer's protocol and added to the membranes in a dark room for 5 min. The solution was subsequently removed, the blots were covered with a flat layer of cellophane and were placed into the imaging system (Tanon 5200; Tanon Science and Technology Co., Ltd.) for scanning. Western blotting was performed in triplicate. ImageJ software version 1.53a (National Institutes of Health) was used to analyze the results and normalize all target proteins to β-actin.

Statistical analysis. GraphPad Prism version 9.5.1 (Dotmatics) was used for statistical analysis. Continuous variables are presented as the mean ± the standard error of the mean. Differences between multiple groups were analyzed using a one-way ANOVA followed by post hoc Tukey test. $P<0.05$ was considered to indicate a statistically significant difference.

Results

LPS induces intestinal epithelial cell injury. To investigate the role of LPS in intestinal epithelial cells, cell viability was assessed using the CCK-8 assay after treatment of cells with different concentrations of LPS. Based on previous literature, reference concentrations for LPS were 0.05-50 μg/ml for 8-48 h (19,23), and for IPA were 0.01-10.0 mM for 24-72 h (24-26). IPA was also observed to induce a dose-dependent suppression of the aggregation of denatured proteins in cells experiencing endoplasmic reticulum stress (25). Therefore, in the present study, NCM460 cells were pre-stimulated with 0-10 μg/ml LPS for 3 and 24 h, followed by treatment with 0.05, 0.5 or 5 mM IPA for 72 h to explore its effect on LPS-induced intestinal epithelial cell injury. The findings indicated that LPS concentrations ranging between 0 and 10 μg/ml did not significantly affect the viability of intestinal epithelial cells following a 3-h treatment ($P>0.05$; Fig. 1A). Notably, there was a sharp decrease in cell viability after 24 h of exposure. The decrease in cell viability was particularly significant when the LPS concentration was >1.0 μg/ml, and the decline was most prominent at 10 μg/ml. These results indicated that specific LPS concentrations may reduce the viability of intestinal epithelial cells, and treatment with 10 μg/ml LPS for 24 h was determined to be the appropriate concentration of LPS that was used for further experiments ($P<0.0001$; Fig. 1B). Subsequently, NCM460 cells were pre-stimulated with LPS, and then treated with different concentrations of IPA for 72 h and a CCK-8 assay was performed. The results showed that LPS-induced NCM460 cells treated with IPA resulted in a dose-dependent increase in cell viability compared with that in the LPS group ($P<0.001$; Fig. 1C).

IPA inhibits the LPS-induced apoptosis of intestinal epithelial cells. To evaluate the effects of IPA on LPS-induced cell injury, the apoptosis of intestinal epithelial cells treated with LPS alone or in combination with various concentrations of IPA was subsequently analyzed. Compared with in the control group, the LPS group exhibited a significant increase in the proportion of apoptotic intestinal epithelial cells ($P<0.0001$; Fig. 2A-C). By contrast, the LPS + IPA groups exhibited a marked reduction in the number of apoptotic cells in a concentration-dependent manner compared with that in the LPS group ($P<0.0001$; Fig. 2A and C-F). These findings demonstrated the effective inhibition of LPS-induced apoptosis in intestinal epithelial cells by IPA. IPA exerted a protective effect on injured intestinal epithelial cells by preventing LPS-induced apoptosis.

IPA improves intestinal epithelial barrier function. To assess the effects of IPA on intestinal barrier function, TEER values were measured. The results showed that LPS significantly reduced TEER as compared to control group ($P<0.0001$), indicating impairment of the barrier function in intestinal epithelial cells (Fig. 3A). By contrast, treatment with IPA alleviated LPS-induced impairment ($P<0.05$). Treatment with low (0.05 mM), medium (0.5 mM) and high (5 mM) concentrations of IPA all significantly increased TEER values in a concentration-dependent manner compared with in the LPS group ($P<0.05$).

It is well established that compromised intestinal barrier integrity can lead to the activation of local immunity and alterations in the structure of TJ proteins (27). To explore the potential impact of IPA on intercellular TJs, the expression of TJ-associated proteins was examined using western blotting. The findings revealed a significant decrease in the expression levels of claudin-1, occludin and ZO-1 in the LPS group compared with those in the control group ($P<0.01$; Fig. 3B-E). However, only treatment with a high concentration of IPA significantly reversed the LPS-induced reduction in the expression levels of these proteins ($P<0.05$) when compared with the LPS group.

To further validate these findings, immunofluorescence analysis of ZO-1 was performed. The results showed that the expression of ZO-1 in the LPS-induced group was significantly decreased compared with that in the control group ($P<0.001$), and there was a substantial increase in ZO-1 protein secretion in both the medium and high concentration IPA-treated cells ($P<0.01$; Fig. 3F and G). Collectively, these findings suggested that IPA may improve the barrier function of intestinal epithelial cells injured by LPS by increasing TEER values and upregulating the expression of TJ proteins.

IPA inhibits the levels of LPS-induced pro-inflammatory cytokines. RT-qPCR was used to investigate the expression levels of pro-inflammatory cytokines in intestinal epithelial cells. Following treatment with LPS, there was a significant increase in the mRNA expression levels of IL-1β, IL-6 and TNF-α

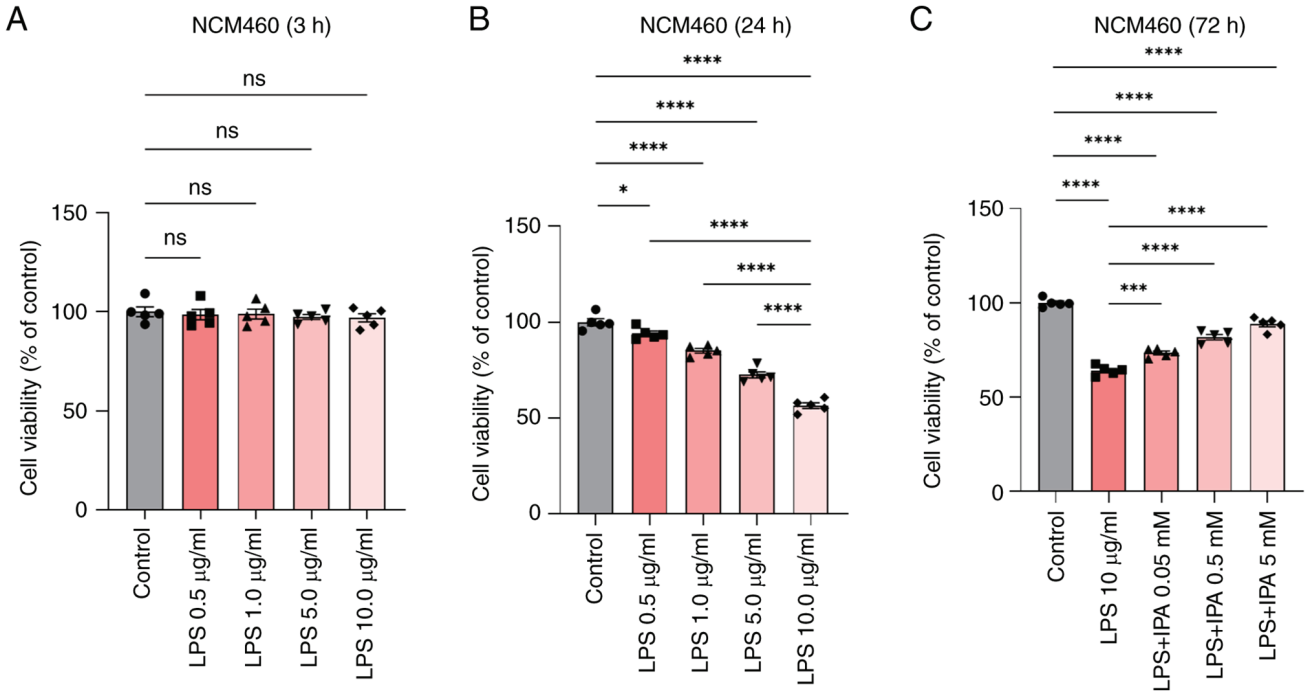

Figure 1. IPA reverses the LPS-induced decrease in the viability of NCM460 cells. Viability of NCM460 cells after treatment with 0, 0.5, 1, 5, or 10 μg/ml LPS for (A) 3 or (B) 24 h. (C) Viability of NCM460 cells treated with 10 μg/ml LPS in combination with various concentrations of IPA for 72 h. Cell viability was determined using the Cell Counting Kit-8 assay. Data are presented as the mean ± SEM, n=5. *P<0.05, ***P<0.001, ****P<0.0001. IPA, indole-3-propionic acid; LPS, lipopolysaccharide.

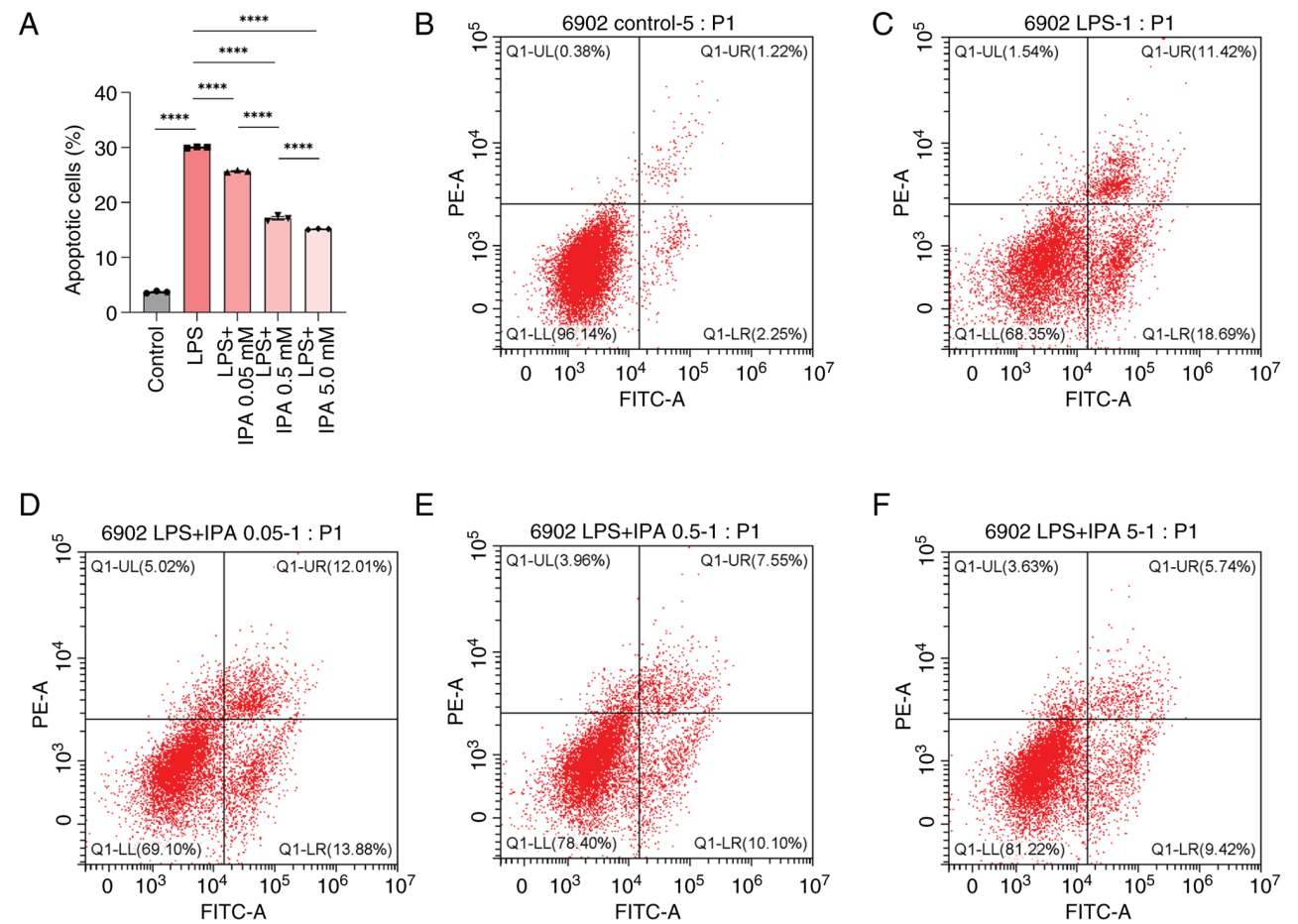

Figure 2. IPA inhibits LPS-induced apoptosis in intestinal epithelial cells. (A) Mean apoptosis rate of NCM460 cells in each group. Representative dot plots of apoptosis analysis by flow cytometry in the (B) control group, (C) LPS group, (D) LPS + 0.05 mM IPA group, (E) LPS + 0.5 mM IPA group and (F) LPS + 5 mM IPA group. Data are presented as mean ± SEM, n=3. ****P<0.0001. IPA, indole-3-propionic acid; LPS, lipopolysaccharide.

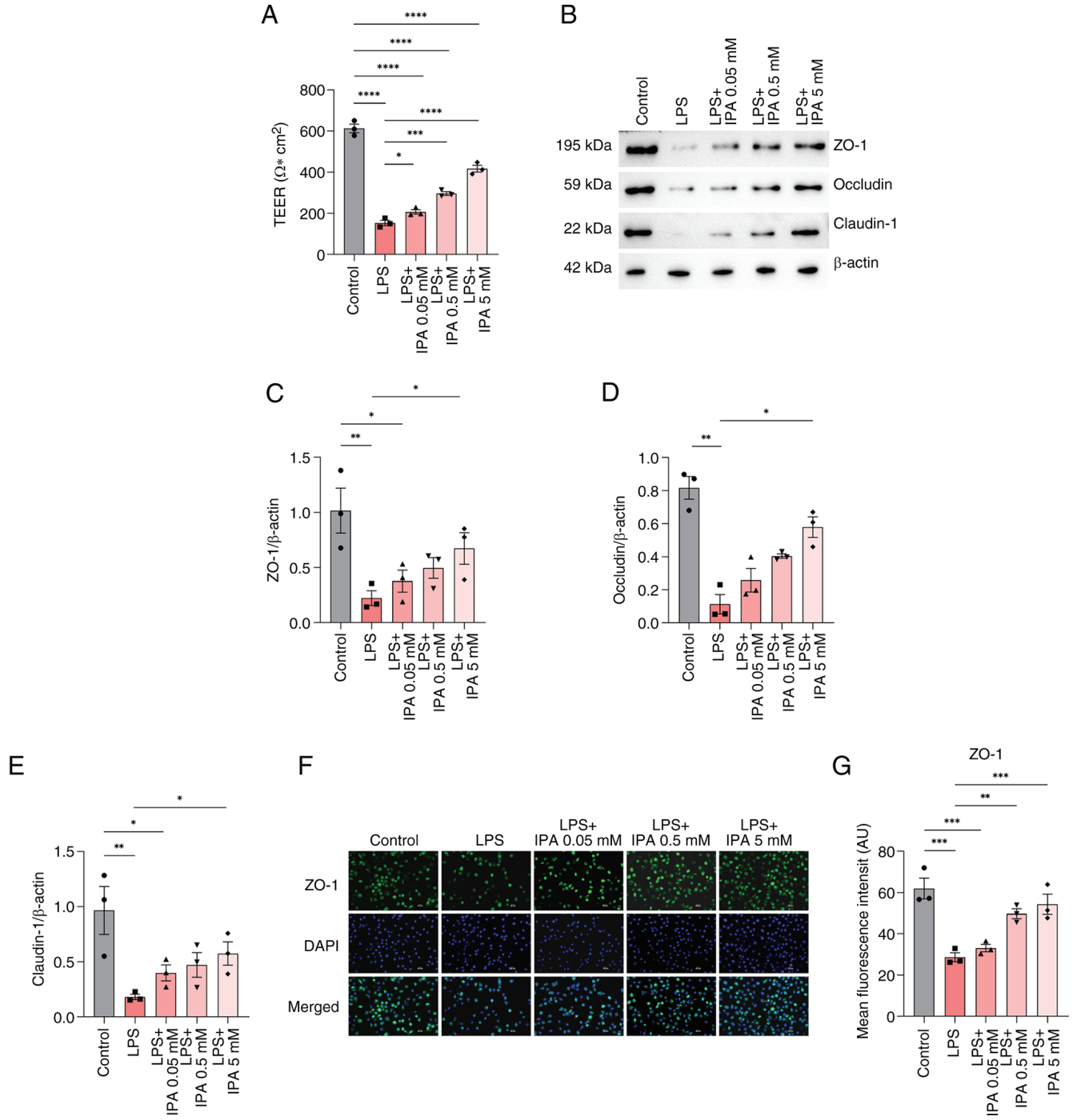

Figure 3. Effects of IPA on the intestinal barrier function in cells treated with LPS. (A) TEER values of the human-derived NCM460 colonic epithelial cells in the different groups. (B) Western blotting, and relative levels of (C) ZO-1, (D) occludin and (E) claudin-1 proteins. (F) Immunofluorescence staining of ZO-1 (green) and nuclei (blue). Scale bars, 50 μm. Magnification, x200. (G) Semi-quantitative analysis of the fluorescence intensity of ZO-1. Data are presented as mean ± SEM, n=3. *P<0.05, **P<0.001, ***P<0.001, ****P<0.0001. IPA, indole-3-propionic acid; LPS, lipopolysaccharide; TEER, transepithelial electrical resistance; ZO-1, zonula occludens-1.

relative to the control group (P<0.0001; Fig. 4A-C). However, IPA treatment resulted in a concentration-dependent down-regulation in IL-1β, IL-6 and TNF-α mRNA expression levels compared with those in the LPS group (P<0.05). Furthermore, the mRNA expression levels of IL-1β, IL-6 and TNF-α were significantly reduced in cells treated with 5 mM IPA compared with in cells treated with 0.05 or 0.5 mM IPA (P<0.05). In addition, the levels of IL-1β, IL-6 and TNF-α secreted by NCM460 cells were analyzed by ELISA. It was similarly observed that IL-1β, IL-6 and TNF-α levels were increased in response to LPS stimulation and were downregulated when cells were also treated with IPA (P<0.05; Fig. 4D-F). These findings collectively indicated that IPA could mitigate LPS-induced pro-inflammatory cytokine expression.

IPA protects intestinal epithelial cells from LPS-induced inflammatory injury via regulation of the TLR4/NF-κB pathway. Activation of the NF-κB pathway has previously been

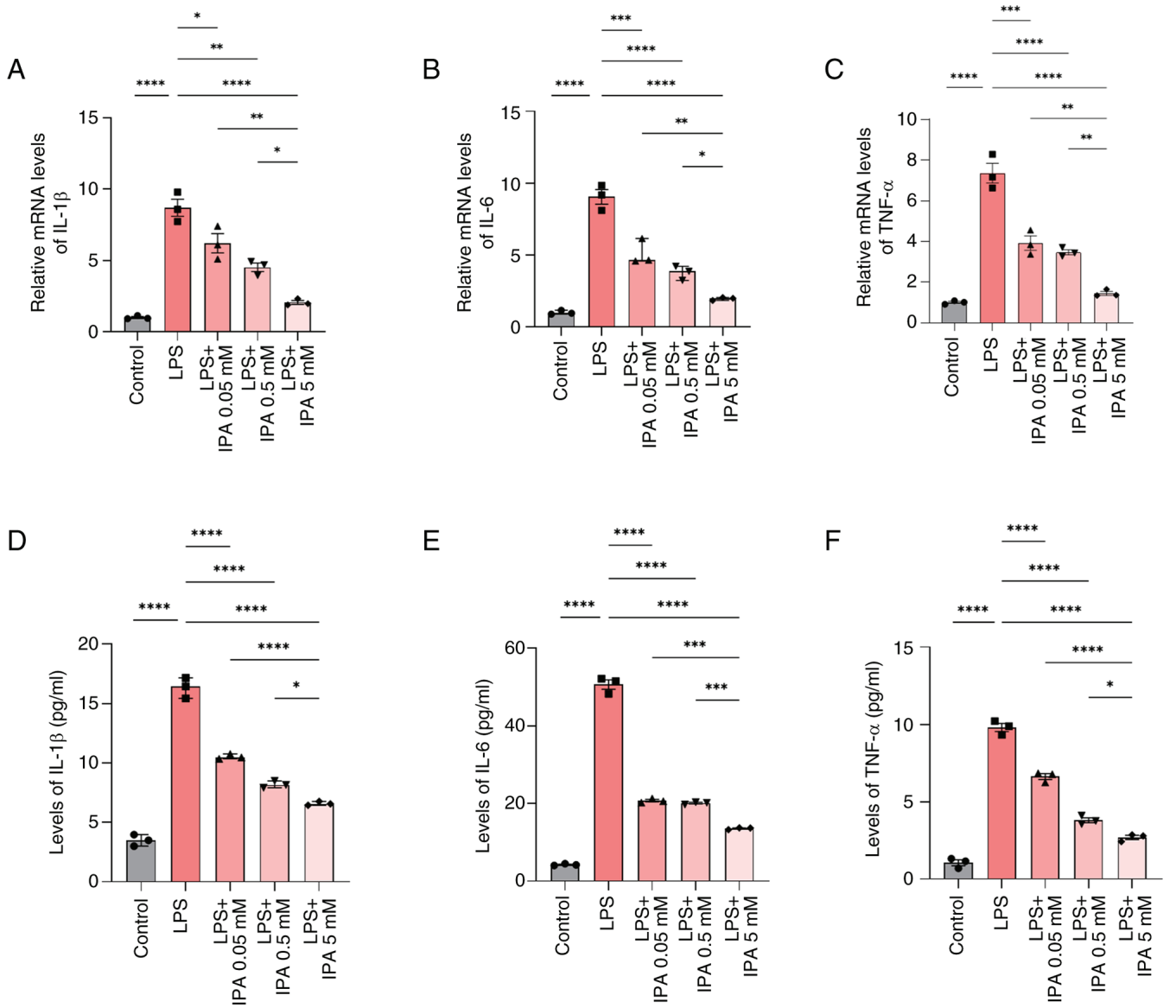

Figure 4. Effect of IPA on LPS-induced pro-inflammatory cytokines. mRNA expression levels of the pro-inflammatory cytokines (A) IL-1β, (B) IL-6 and (C) TNF-α were detected by reverse transcription-quantitative PCR. Enzyme-linked immunosorbent assay was used to detect the levels of (D) IL-1β, (E) IL-6 and (F) TNF-α. Data are presented as mean ± SEM, n=3. *P<0.05, **P<0.01, ***P<0.001, ****P<0.0001. IPA, indole-3-propionic acid; LPS, lipopolysaccharide.

implicated in the maintenance of intestinal barrier integrity in response to LPS-induced injury accompanied by the release of pro-inflammatory cytokines (22). LPS activates TLR4 and NF-κB signaling pathways sequentially, ultimately resulting in the release of large quantities of pro-inflammatory cytokines, including IL-6, IL-1β and TNF-α (23). Western blotting was performed to examine the effects of IPA on p65-NF-κB expression. The results showed that phosphorylation of p65-NF-κB was significantly increased in the LPS group compared with that in the control group (P<0.0001), which was reversed by treatment with IPA in a dose-dependent manner (P<0.001; Fig. 5A and B).

The effect of IPA on the inhibition of p65-NF-κB was validated using a dual-luciferase reporter gene assay system, and the results were similar to those observed using western blotting. Compared with in the LPS group, treatment with IPA effectively inhibited the activation of p65-NF-κB in a concentration-gradient dependent manner (P<0.0001), and high-concentration IPA showed optimal inhibition in comparison with the low-concentration group (P<0.0001; Fig. 5C).

To gain further insights into the mechanism underlying IPA-mediated inhibition of p65-NF-κB, the mRNA expression levels of key proteins in the NF-κB signaling pathway were examined by RT-qPCR. The mRNA expression levels of TLR4, NF-κB, MyD88 and TRIF were significantly higher in the LPS group compared with those in the control group (P<0.0001); however, in the presence of IPA, the expression levels of these genes were reduced in a concentration-dependent manner compared with those in the LPS group (P<0.05; Fig. 5D-G). These results indicated that IPA exerted a regulatory effect on both the TLR4/MyD88/NF-κB signaling pathway and the TLR4/TRIF/NF-κB signaling pathway, thereby inhibiting the release of pro-inflammatory cytokines and protecting intestinal epithelial cells against LPS-induced inflammatory injury. Taken together, these results suggested that IPA may hold promise for mitigating the detrimental effects of inflammation in the gut.

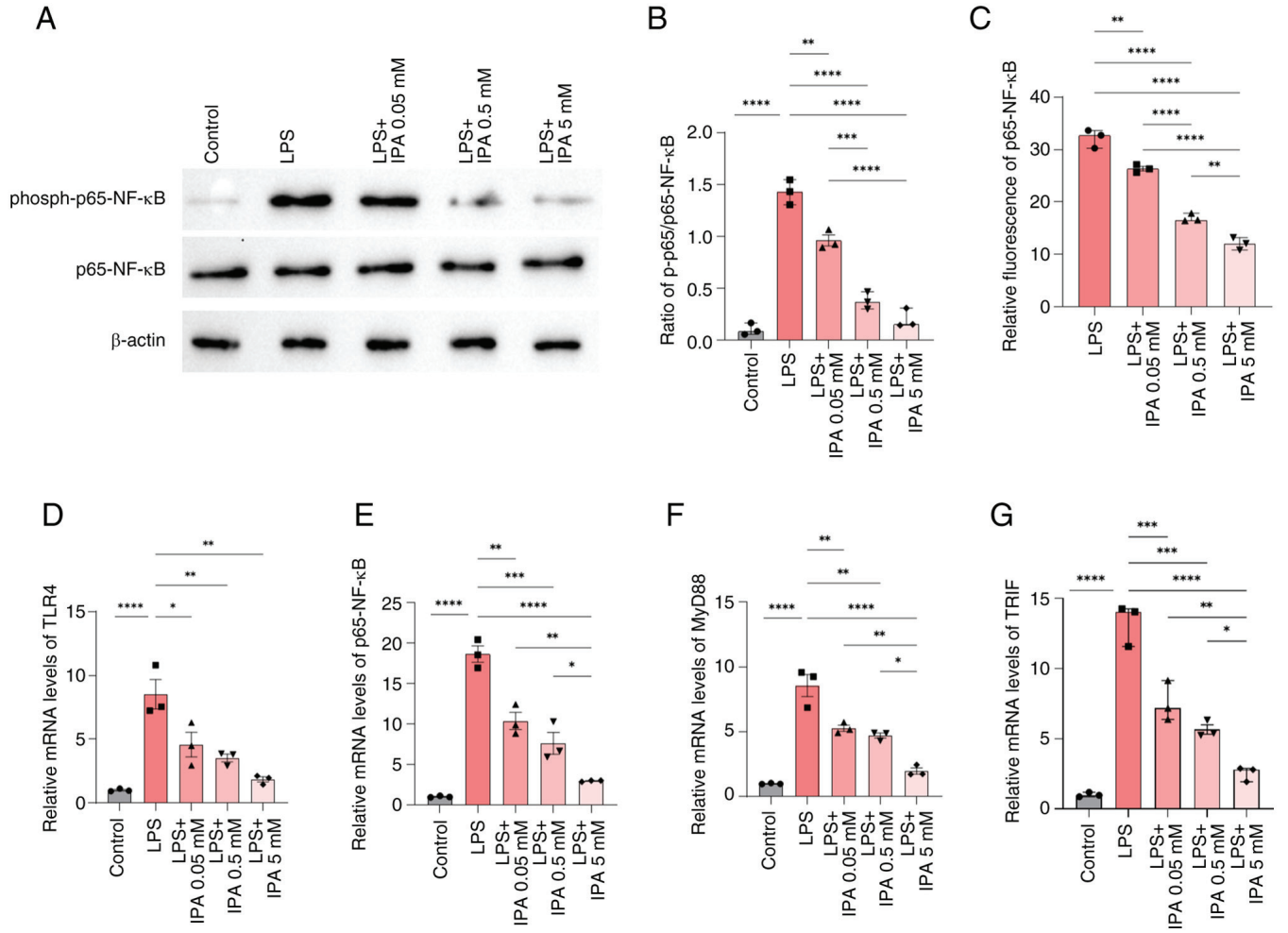

Figure 5. IPA improves intestinal epithelial barrier function via regulation of the NF-κB pathway. (A) Representative blots of p65-NF-κB and phospho-p65-NF-κB expression. (B) Ratio of phospho-p65/p65-NF-κB based on the results of western blotting. (C) Effect of IPA on the bioactivity of p65-NF-κB using a dual-luciferase reporter assay. (D) TLR4, (E) p65-NF-κB, (F) MyD88 and (G) TRIF mRNA expression levels were determined by reverse transcription-quantitative PCR. Data are presented as the mean ± SEM, n=3. *P<0.05, **P<0.01, ***P<0.001, ****P<0.0001. IPA, indole-3-propionic acid; LPS, lipopolysaccharide; MyD88, myeloid differentiation factor 88; phospho, phosphorylated; TLR4, Toll-like receptor 4.

Discussion

Intestinal epithelial cells serve an important role in maintaining a strong epithelial barrier and thus maintaining good health (10). Previous studies have demonstrated the toxic effects of high doses of LPS on cells (23,28,29). In the present study, treatment with 1 μg/ml LPS for 24 h reduced cell viability, with the maximal effect observed in response to 10 μg/ml LPS, resulting in the significant induction of apoptosis of intestinal epithelial cells. IPA exerted an inhibitory effect on LPS-induced intestinal epithelial cell dysfunction, which is consistent with previous research (29). The present study demonstrated that LPS reduced TEER and the expression levels of TJ proteins in NCM460 cells; however, IPA treatment alleviated the effects of LPS, highlighting the protective effects of IPA on LPS-induced intestinal barrier dysfunction *in vitro*.

TJ proteins have a crucial role in forming cell-to-cell interactions and serve as the primary defensive barrier of the intestinal epithelium (30). Abrogating TJ protein structure can lead to disruption of the barrier integrity, resulting in changes in intestinal epithelial cell permeability, and thus the subsequent development of various diseases associated with intestinal mucosal inflammation (31). TJ proteins consist of transmembrane proteins, such as occludin and claudin; cytoplasmic proteins, such as ZOs and cingulin; and cytoskeletal proteins, such as actin and myosin (32). Studies have shown that intestinal injury is associated with the reduced expression and translocation of TJ proteins (27,29,33,34). Research on enterocyte cells has demonstrated that IPA can improve barrier properties by increasing the expression of TJ proteins and other junction proteins (11). Additionally, in rats fed a high-fat diet, it was shown that IPA treatment restored the height of villi in the ileum, and promoted the expression of ZO-1, occludin and claudin-1 (29). In the present study, treatment with a high concentration (5 mM) of IPA significantly reversed the decrease in the expression levels of claudin-1, occludin and ZO-1 in NCM460 cells with LPS-induced intestinal epithelial injury, indicating that higher concentrations of IPA improve intestinal barrier function. Subsequent semi-quantitative immunofluorescence analysis of ZO-1 protein expression demonstrated that not only a high concentration (5 mM) of IPA, but also a medium concentration (0.5 mM) of IPA, effectively

reversed the LPS-induced decrease in ZO-1 expression. The difference in the effects of the various concentrations may be due to the assays being used, with immunofluorescence staining focused more on localization, whereas western blotting is used to assess total cellular protein. However, both approaches indicated that the expression of the TJ protein ZO-1 in the LPS-induced group was significantly decreased compared with that in the control group, and that IPA up to a certain concentration was effective in reversing the LPS-induced reduction in the expression of ZO-1. Strategies targeting TJ proteins, such as claudin-binding and angulin-binding agents, and their application in drug development have been the focus of research into novel therapeutics in previous years (27). However, the present study was mainly limited to ZO-1, and future studies should focus on other TJ proteins, including claudins, occludin, tricellulin, angulins and junctional adhesion molecules to fully evaluate the mechanism of the action of IPA on TJ proteins. Moreover, further refinement and assessment of IPA concentrations should be investigated.

The disruption of intestinal barrier integrity can lead to activation of local immunity and can result in an imbalance of cytokines. However, there is evidence to suggest that IPA can regulate intestinal permeability and barrier function during inflammation by downregulating TNF-α in intestinal cells (29). Furthermore, another study reported that IPA can activate the transcription factor aryl hydrocarbon receptor in response to the production of byproducts from commensals (35), thereby maintaining intestinal homeostasis and regulating immunity (36). Additionally, IPA has been found to reduce the levels of proinflammatory factors and to improve intestinal histopathology (10). Nonetheless, studies characterizing the mechanisms of IPA in LPS-induced intestinal epithelial cell injury are still lacking. It is well established that LPS can trigger downstream MyD88/NF-κB signals via activation of TLR4, leading to the production of proinflammatory cytokines (16,37). Consistently, the results of the present study revealed that genes related to the TLR4/NF-κB signaling pathway were significantly upregulated following LPS intervention. By contrast, IPA reduced the phosphorylation levels of p65-NF-κB in LPS-induced cells, as well as the levels of pro-inflammatory cytokines, including IL-1β, IL-6 and TNF-α. These findings suggested that IPA inhibited the release of pro-inflammatory cytokines (IL-1β, IL-6 and TNF-α) in a concentration-dependent manner via regulation of the TLR4/MyD88/NF-κB and TLR4/TRIF/NF-κB pathways, and thereby alleviated LPS-induced inflammatory injury in human colonic epithelial cells. The present study provides valuable insights into the therapeutic potential of IPA in alleviating LPS-induced inflammatory injury.

The present study has some limitations. The protective effects of IPA were only assessed in NCM460 cells; thus, additional studies in other colonic epithelial cells are required. Further experiments to detect additional TJ proteins, including tricellulin and junctional adhesion molecules, may also better reveal the interactive mechanism between IPA and intestinal barrier integrity. Moreover, animal experiments were not performed to determine if the mechanism identified was observed *in vivo*. However, the results of the current *in vitro* study may improve the understanding of the mechanism of action of IPA on alleviating the inflammatory response induced by LPS and improving intestinal barrier function. In future studies, additional *in vitro* experiments using other cell lines and *in vivo* experiments are required to validate the findings of the present study.

In conclusion, the present study provides compelling evidence for the protective effects of IPA on LPS-induced intestinal epithelial cell injury and intestinal barrier function *in vitro*. This was accompanied by the suppression of the expression of TLR4, and downstream adaptor proteins MyD88 and TRIF, as well as the inhibition of NF-κB. These findings shed light on the potential therapeutic value of IPA in diseases characterized by LPS-induced intestinal epithelial cell inflammatory injury and intestinal barrier dysfunction. Nevertheless, further studies are warranted to explore the precise mechanisms and optimal concentration through which IPA exerts its protective effects and to evaluate its efficacy in clinical settings.

Acknowledgements

Not applicable.

Funding

This study was supported by the Shanghai Minhang District Natural Science Foundation (grant no. 2022MHZ028) to YC and the Disciplinary Construction Project of Minhang Hospital (grant no. YJXK-2021-08) to SC. The funders had no role in the study design, data collection and analysis, decision to publish, or manuscript preparation.

Availability of data and materials

The data generated in the present study may be requested from the corresponding author.

Authors' contributions

YL, YC and WC carried out the experiments, participated in collecting data and drafted the manuscript. XL and QF performed the statistical analysis and participated in its design. FL and SC participated in acquisition, analysis or interpretation of data, and drafted the manuscript. YL and YC confirm the authenticity of all the raw data. All authors read and approved the final version of the manuscript.

Ethics approval and consent to participate

Not applicable.

Patient consent for publication

Not applicable.

Competing interests

The authors declare that they have no competing interests.

References

1. Wlodarska M, Luo C, Kolde R, d'Hennezel E, Annand JW, Heim CE, Krastel P, Schmitt EK, Omar AS, Creasey EA, *et al*: Indoleacrylic acid produced by commensal peptostreptococcus species suppresses inflammation. Cell Host Microbe 22: 25-37. e6, 2017.
2. Wan F, Wang M, Zhong R, Chen L, Han H, Liu L, Zhao Y, Lv H, Hou F, Yi B and Zhang H: Supplementation With chinese medicinal plant extracts from lonicera hypoglauca and scutellaria baicalensis mitigates colonic inflammation by regulating oxidative stress and gut microbiota in a colitis mouse model. Front Cell Infect Microbiol 11: 798052, 2022.
3. Xu QQ, Su ZR, Yang W, Zhong M, Xian YF and Lin ZX: Patchouli alcohol attenuates the cognitive deficits in a transgenic mouse model of Alzheimer's disease via modulating neuropathology and gut microbiota through suppressing C/EBPβ/AEP pathway. J Neuroinflammation 20: 19, 2023.
4. Wang Z, Cao Y, Zhang K, Guo Z, Liu Y, Zhou P, Liu Z and Lu X: Gold nanoparticles alleviates the lipopolysaccharide-induced intestinal epithelial barrier dysfunction. Bioengineered 12: 6472-6483, 2021.
5. Wang Y, Lin J, Cheng Z, Wang T, Chen J and Long M: Bacillus coagulans TL3 inhibits LPS-induced caecum damage in rat by regulating the TLR4/MyD88/NF-κB and Nrf2 signal pathways and modulating intestinal microflora. Oxid Med Cell Longev 2022: 5463290, 2022.
6. Hasain Z, Che Roos NA, Rahmat F, Mustapa M, Raja Ali RA and Mokhtar NM: Diet and pre-intervention washout modifies the effects of probiotics on gestational diabetes mellitus: A comprehensive systematic review and meta-analysis of randomized controlled trials. Nutrients 13: 3045, 2021.
7. Knudsen C, Neyrinck AM, Leyrolle Q, Baldin P, Leclercq S, Rodriguez J, Beaumont M, Cani PD, Bindels LB, Lanthier N and Delzenne N: Hepatoprotective effects of indole, a gut microbial metabolite, in leptin-deficient obese mice. J Nutr 151: 1507-1516, 2021.
8. Konopelski P and Ufnal M: Indoles-gut bacteria metabolites of tryptophan with pharmacotherapeutic potential. Curr Drug Metab 19: 883-890, 2018.
9. Liu Q, Yu Z, Tian F, Zhao J, Zhang H, Zhai Q and Chen W: Surface components and metabolites of probiotics for regulation of intestinal epithelial barrier. Microb Cell Fact 19: 23, 2020.
10. Alexeev EE, Lanis JM, Kao DJ, Campbell EL, Kelly CJ, Battista KD, Gerich ME, Jenkins BR, Walk ST, Kominsky DJ and Colgan SP: Microbiota-derived indole metabolites promote human and murine intestinal homeostasis through regulation of interleukin-10 receptor. Am J Pathol 188: 1183-1194, 2018.
11. Li J, Zhang L, Wu T, Li Y, Zhou X and Ruan Z: Indole-3-propionic acid improved the intestinal barrier by enhancing epithelial barrier and mucus barrier. J Agric Food Chem 69: 1487-1495, 2021.
12. Wu Y, Li J, Ding W, Ruan Z and Zhang L: Enhanced intestinal barriers by puerarin in combination with tryptophan. J Agric Food Chem 69: 15575-15584, 2021.
13. He S, Wang J, Huang Y, Kong F, Yang R, Zhan Y, Li Z, Ye C, Meng L, Ren Y, *et al*: Intestinal fibrosis in aganglionic segment of Hirschsprung's disease revealed by single-cell RNA sequencing. Clin Transl Med 13: e1193, 2023.
14. Yu YH, Lai YH, Hsiao FS and Cheng YH: Effects of deoxynivalenol and mycotoxin adsorbent agents on mitogen-activated protein kinase signaling pathways and inflammation-associated gene expression in porcine intestinal epithelial cells. Toxins (Basel) 13: 301, 2021.
15. Chen X, Liu G, Yuan Y, Wu G, Wang S and Yuan L: NEK7 interacts with NLRP3 to modulate the pyroptosis in inflammatory bowel disease via NF-κB signaling. Cell Death Dis 10: 906, 2019.
16. Zeng S, Li W, Ouyang H, Xie Y, Feng X and Huang L: A novel prognostic pyroptosis-related gene signature correlates to oxidative stress and immune-related features in gliomas. Oxid Med Cell Longev 2023: 4256116, 2023.
17. Pulakazhi Venu VK, Saifeddine M, Mihara K, Tsai YC, Nieves K, Alston L, Mani S, McCoy KD, Hollenberg MD and Hirota SA: The pregnane X receptor and its microbiota-derived ligand indole 3-propionic acid regulate endothelium-dependent vasodilation. Am J Physiol Endocrinol Metab 317: E350-E361, 2019.
18. Venkatesh M, Mukherjee S, Wang H, Li H, Sun K, Benechet AP, Qiu Z, Maher L, Redinbo MR, Phillips RS, *et al*: Symbiotic bacterial metabolites regulate gastrointestinal barrier function via the xenobiotic sensor PXR and Toll-like receptor 4. Immunity 41: 296-310, 2014.
19. Wang Y, Xi W, Zhang X, Bi X, Liu B, Zheng X and Chi X: CTSB promotes sepsis-induced acute kidney injury through activating mitochondrial apoptosis pathway. Front Immunol 13: 1053754, 2023.
20. Ismael S, Rodrigues C, Santos GM, Castela I, Mota IB, Barreiros-Mota I, Almeida MJ, Calhau C, Faria A and Araújo JR: IPA and its precursors differently modulate the proliferation, differentiation, and integrity of intestinal epithelial cells. Nutr Res Pract 17: 616-630, 2023.
21. Guo C, Guo D, Fang L, Sang T, Wu J, Guo C, Wang Y, Wang Y, Chen C, Chen J, *et al*: Ganoderma lucidum polysaccharide modulates gut microbiota and immune cell function to inhibit inflammation and tumorigenesis in colon. Carbohydr Polym 267: 118231, 2021.
22. Livak KJ and Schmittgen TD: Analysis of relative gene expression data using real-time quantitative PCR and the 2(-Delta Delta C(T)) method. Methods 25: 402-408, 2001.
23. Zhou Y, Duan L, Zeng Y, Song X, Pan K, Niu L, Pu Y, Li J, Khalique A, Fang J, *et al*: The panda-derived lactiplantibacillus plantarum BSG201683 improves LPS-induced intestinal inflammation and epithelial barrier disruption in vitro. BMC Microbiol 23: 249, 2023.
24. Sehgal R, Ilha M, Vaittinen M, Kaminska D, Männistö V, Kärjä V, Tuomainen M, Hanhineva K, Romeo S, Pajukanta P, *et al*: Indole-3-propionic acid, a gut-derived tryptophan metabolite, associates with hepatic fibrosis. Nutrients 13: 3509, 2021.
25. Mimori S, Kawada K, Saito R, Takahashi M, Mizoi K, Okuma Y, Hosokawa M and Kanzaki T: Indole-3-propionic acid has chemical chaperone activity and suppresses endoplasmic reticulum stress-induced neuronal cell death. Biochem Biophys Res Commun 517: 623-628, 2019.
26. Zhang B, Jiang M, Zhao J, Song Y, Du W and Shi J: The mechanism underlying the influence of indole-3-propionic acid: A relevance to metabolic disorders. Front Endocrinol (Lausanne) 13: 841703, 2022.
27. Hashimoto Y, Tachibana K, Krug SM, Kunisawa J, Fromm M and Kondoh M: Potential for tight junction protein-directed drug development using claudin binders and angubindin-1. Int J Mol Sci 20: 4016, 2019.
28. Su Y, Chen C, Guo L, Du J, Li X and Liu Y: Ecological balance of oral microbiota is required to maintain oral mesenchymal stem cell homeostasis. Stem Cells 36: 551-561, 2018.
29. Zhao ZH, Xin FZ, Xue Y, Hu Z, Han Y, Ma F, Zhou D, Liu XL, Cui A, Liu Z, *et al*: Indole-3-propionic acid inhibits gut dysbiosis and endotoxin leakage to attenuate steatohepatitis in rats. Exp Mol Med 51: 1-14, 2019.
30. Mu Q, Kirby J, Reilly CM and Luo XM: Leaky gut as a danger signal for autoimmune diseases. Front Immunol 8: 598, 2017.
31. Shi R, Yu F, Hu X, Liu Y, Jin Y, Ren H, Lu S, Guo J, Chang J, Li Y, *et al*: Protective effect of lactiplantibacillus plantarum subsp. Plantarum SC-5 on dextran sulfate sodium-induced colitis in mice. Foods 12: 897, 2023.
32. Zhao X, Zeng H, Lei L, Tong X, Yang L, Yang Y, Li S, Zhou Y, Luo L, Huang J, *et al*: Tight junctions and their regulation by non-coding RNAs. Int J Biol Sci 17: 712-727, 2021.
33. He C, Deng J, Hu X, Zhou S, Wu J, Xiao D, Darko KO, Huang Y, Tao T, Peng M, *et al*: Vitamin A inhibits the action of LPS on the intestinal epithelial barrier function and tight junction proteins. Food Funct 10: 1235-1242, 2019.
34. Stephens M and von der Weid PY: Lipopolysaccharides modulate intestinal epithelial permeability and inflammation in a species-specific manner. Gut Microbes 11: 421-432, 2020.
35. Rothhammer V, Mascanfroni ID, Bunse L, Takenaka MC, Kenison JE, Mayo L, Chao CC, Patel B, Yan R, Blain M, *et al*: Type I interferons and microbial metabolites of tryptophan modulate astrocyte activity and central nervous system inflammation via the aryl hydrocarbon receptor. Nat Med 22: 586-597, 2016.
36. Hubbard TD, Murray IA and Perdew GH: Indole and tryptophan metabolism: Endogenous and dietary routes to Ah receptor activation. Drug Metab Dispos 43: 1522-1535, 2015.
37. Huang X, Zhu J, Jiang Y, Xu C, Lv Q, Yu D, Shi K, Ruan Z and Wang Y: SU5416 attenuated lipopolysaccharide-induced acute lung injury in mice by modulating properties of vascular endothelial cells. Drug Des Devel Ther 13: 1763-1772, 2019.